Chemistry & Biology
Article

Spin-Labeled Analogs of CMP-NeuAc as NMR Probes of the α-2,6-Sialyltransferase ST6Gal I

Shan Liu,[1] Andre Venot,[1] Lu Meng,[1] Fang Tian,[1] Kelley W. Moremen,[1] Geert-Jan Boons,[1] and James H. Prestegard[1,*]
[1] Complex Carbohydrate Research Center, University of Georgia, Athens, GA 30602, USA
*Correspondence: jpresteg@ccrc.uga.edu
DOI 10.1016/j.chembiol.2007.02.010

SUMMARY

Structural data on mammalian proteins are often difficult to obtain by conventional NMR approaches because of an inability to produce samples with uniform isotope labeling in bacterial expression hosts. Proteins with sparse isotope labels can be produced in eukaryotic hosts by using isotope-labeled forms of specific amino acids, but structural analysis then requires information from experiments other than nuclear Overhauser effects. One source of alternate structural information is distance-dependent perturbation of spin relaxation times by nitroxide spin-labeled analogs of natural protein ligands. Here, we introduce spin-labeled analogs of sugar nucleotide donors for sialyltransferases, specifically, CMP-TEMPO (CMP-4-*O*-[2,2,6,6-tetramethylpiperidine-1-oxyl]) and CMP-4carboxyTEMPO (CMP-4-*O*-[4-carboxy-2,2,6,6-tetramethylpiperidinine-1-oxyl]). An ability to identify resonances from active site residues and produce distance constraints is illustrated on a ^{15}N phenylalanine-labeled version of the structurally uncharacterized, α-2,6-linked sialyltransferase, ST6Gal I.

INTRODUCTION

Structural determination of proteins by NMR methods has traditionally relied on the detection of large numbers of nuclear Overhauser effects (NOEs). Uniform labeling with ^{13}C, ^{15}N, and ^{2}H provides the improved resolution necessary for the assignment of sufficient numbers of resonances to conduct an NOE-based structure determination [1, 2]. The labeling is usually accomplished by expressing proteins in bacterial hosts that efficiently utilize low-cost ^{13}C- and ^{15}N-enriched substrates. However, there are many proteins for which bacterial expression is not practical. For example, proteins that require glycosylation for proper folding or full activity are normally expressed in eukaryotic hosts that require supplementation with a nearly complete set of labeled amino acids, some of which are very expensive [3, 4]. This is not a small class of proteins. About 50% of mammalian proteins may be glycosylated [5]. It is therefore important to consider alternate sources of structural data that can be used with the sparse labels introduced by expressing proteins in eukaryotic cells grown on media supplemented with selected sets of less expensive ^{15}N-labeled amino acids [6]. One source applicable to this type of labeling relies on paramagnetic perturbation of labeled sites upon introducing nitroxide-carrying probes that are either substrate mimics or are covalently attached to the protein itself [7–15]. Here, we present a probe that mimics a sugar nucleotide binding to the active site of a glycosyltransferase. The protein target is the structurally uncharacterized sialyltransferase, ST6Gal I, a protein that is itself glycosylated [16]. The sugar nucleotide mimicked is the sialic acid-carrying CMP-NeuAc. The mimic is demonstrated to be useful in identifying active site residues of sialyltransferases, and the studies lay groundwork for more general applications to glycosyltransferase structure.

The essential component of the nitroxide spin label we chose is the chemically stable moiety TEMPO (2,2,6,6-tetramethylpiperidine-1-oxyl). The nitroxide group contains an unpaired electron that drastically increases the relaxation of neighboring protons due to the large magnitude of the electron magnetic moment. The interactions between electron and proton magnetic moments extend to 20 Å, a distance much longer than for proton-proton NOEs, which are limited to distances of 6 Å or less [1, 2]. In more quantitative terms, when the nitroxide spin-labeled compound binds to the protein target, the nuclei of protein residues experience enhanced spin relaxation with a $1/r^6$ dependence on the distance, r, between the nitroxide group and the nuclear site [7–15]. Resonances are broadened, longitudinal spin relaxation times are shortened, and crosspeak intensity in most multidimensional experiments is reduced.

Here, we use a simple method for detecting spin relaxation enhancements that depends on intensity loss of crosspeaks in ^{1}H-^{15}N HSQC spectra [7, 12, 13]. The loss is primarily due to transverse relaxation of protons during INEPT transfers to nitrogen and back, and intensity loss can be directly correlated with the inverse sixth power of the distance between the nitroxide group and the protons giving rise to each crosspeak. The general procedure is to acquire a spectrum of the protein with the spin-labeled ligand in its oxidized paramagnetic form, then reduce the nitroxide to a diamagnetic species with an ascorbate salt, and repeat the spectral acquisition under as identical

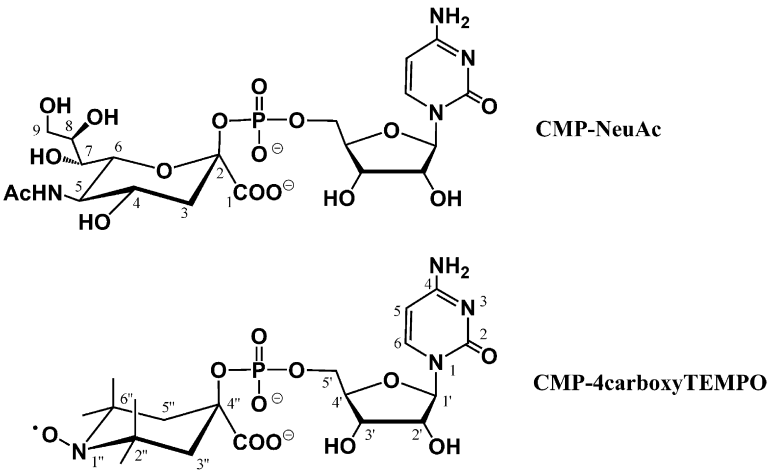

Figure 1. Structure of the Natural Donor CMP-NeuAc and Its Analog CMP-4CarboxyTEMPO

conditions as possible. The difference in crosspeak intensities between the oxidized and reduced spectra should be directly attributable to effects of the nitroxide electron spin. Crosspeaks from protons in the ligand-binding site are easily identified, and distances to protons in more remote sites can be estimated.

ST6Gal I (EC 2.4.99.1) was chosen as the target protein for the development of new structural probes based on its biological significance and its current lack of structural characterization. ST6Gal I catalyzes the transfer of sialic acid residues from its native donor, CMP-NeuAc, to terminal galactose residues of oligosaccharides on mammalian proteins. Variability in the addition of sialic acids to various proteins is correlated with colon cancer, development of brain tumors, and immune regulation in the human body [17, 18].

ST6Gal I is a member of the family 29 glycosyltransferases as defined by the CAZY database (www.cazy.org/CAZY/). This family has no structural representative in the RCSB Protein Data Bank (www.rcsb.org/pdb/). While the structures of two bacterial sialyltransferases, CstII (EC 2.4.99.-) and Δ24PmST1 (EC 2.4.99.4; EC 2.4.99.6; EC 2.4.99.9), are known, the sequence of ST6Gal I (over 321 amino acids) is only 11% and 15% identical, respectively, to these proteins [19, 20]. ST6Gal I has two consensus sites for N-glycosylation (both appear to be used), and it is a type II membrane protein. Both its native glycosylation and status as a membrane protein are likely to have contributed to the lack of structural characterization. The catalytic domain of ST6Gal I was, however, cloned and expressed in mammalian cells as early as 1987 [21], and it is this domain that we focus on here. While refolding of small amounts of insoluble protein expressed in *E. coli* has been reported recently [22], mammalian cell expression remains the preferred means of producing a characterizable amount of active protein. The lack of structural characterization and the difficulties in bacterial host expression make ST6Gal I a prime target for sparse isotopic labeling and use of distance constraints derived from paramagnetic spin relaxation enhancement.

In developing appropriate paramagnetic analogs, we use CMP-NeuAc (Figure 1), the sugar donor in the sialylation reaction catalyzed by ST6Gal I, as a model. The spin label might be introduced to either the nucleotide base or the sugar ring. Previous studies involving the design of sialyltransferase inhibitors show that the cytidine nucleotide portion is more critical for tight binding to sialyltransferases than the neuraminic acid residue [23]. Nucleotide base-modified CMP-NeuAc analogs are not tolerated by α-2,6-sialyltransferase, while sugar-modified analogs with derivatization at C5, C8, or C9 of the neuraminic acid residue show affinities for ST6Gal I [24]. Substitution of the proton at C3 with fluorine leads to another potentially useful inhibitor of sialyltransferases [25]. Therefore, we initiated studies in which TEMPO, the spin-labeled nitroxide moiety, would be linked to the phosphate of CMP through its C4 carbon; thus, TEMPO takes the place of the neuraminic acid in CMP-NeuAc. The six-membered ring of TEMPO mimics the six-membered ring of the neuraminic acid. The additional methyl groups at C2 and C6 in TEMPO sit in the positions occupied by C4 substituents and the C7-C8 extension of neuraminic acid, and the nitroxide replaces the C5 acetyl group of neuraminic acid. To further examine the logic of this replacement, CMP-TEMPO was modeled into the crystal structure of CstII, in which CMP-3FNeuAc occupies the sugar donor site. There are no severe steric conflicts identified. However, there is a noticeable absence of a carboxyl group that apparently interacts with positively charged amino acids in the binding site. Therefore, we also synthesized CMP-4carboxyTEMPO (Figure 1), in which a carboxyl group is attached to C4 of TEMPO and effectively mimics the carboxyl attached to C2 of neuraminic acid. CMP-4carboxyTEMPO is demonstrated here to be a good mimic of CMP-NeuAc and a useful structural probe for ST6Gal I.

RESULTS

Preparation of the Spin-Labeled Ligands CMP-TEMPO, 1, and CMP-4CarboxyTEMPO, 2

The synthesis of TEMPO-phosphate derivatives of steroids [26, 27], TEMPO-modified adenosine diphosphate

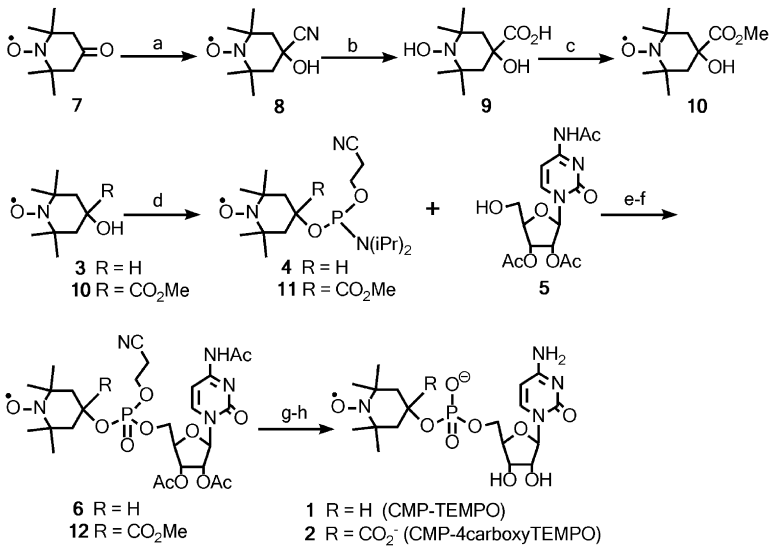

Figure 2. Scheme for the Synthesis of TEMPO Analogs of CMP-NeuAc

Key: (a) 30% H_2SO_4/NaCN, THF, < 15°C. (b) 27% HCl, H_2O, 80°C. (c) CH_2N_2/Et_2O, MeOH. (d) $(iPr)_2NP(Cl)OCH_2CH_2CN$, $Et(iPr)_2N$, CH_2Cl_2. (e) 1H-tetrazole, MeCN, −40°C. (f) t-BuOOH, MeCN. (g) DBU, THF. (h) NaOMe, MeOH-H_2O.

derivatives [28, 29], and TEMPO-modified di- and trideoxy adenylates [30] has been reported. While providing important precedents, the present synthesis of two TEMPO derivatives of CMP-NeuAc, **1** and **2** (Figure 2), is based upon procedures reported for the synthesis of CMP-NeuAc and its analogs [31–34].

The synthesis of **1** started from the available precursor, **3**, while the synthesis of **2** required the preparation of intermediate **10**. Compound **10** was obtained from the commercial 4-Oxo-TEMPO **7** through the known cyanohydrin **8** [35]. Hydrolysis of the nitrile group in strongly acidic conditions [36] provided the acid **9** in which the nitroxide had been reduced. After removal of excess HCl, the crude product was transformed into its methyl ester with diazomethane and slowly reoxidized by air [37, 38] to the nitroxide **10**, which was then purified. The easily prepared phosphoramidite derivatives **4** and **11** [33] were reacted with the primary hydroxyl of the known cytidine derivative **5** [31] in the presence of tetrazole [32]. The obtained intermediate phosphites were directly oxidized with tBuOOH to provide the phosphates **6** and **12**, respectively, which were then purified [32]. As expected, compound **12** was obtained in a lower yield than compound **6**, likely due to the effect of steric hindrance in the intermediate **11**. Careful two-step deprotection of **6** and **12** followed a literature procedure [32] to provide **1** and **2**, respectively.

Determination of Binding Affinities for Spin-Labeled Analogs

An IC_{50} was measured as 8.7 ± 0.1 mM for CMP-TEMPO and 15–20 mM for its reduced form, while an IC_{50} was measured as 1.7 ± 0.1 mM for CMP-4carboxyTEMPO and 3.5 ± 0.1 mM for its reduced form. With the substrate level (S) of 171 μM and a K_M of 150 μM for CMP-NeuAc, the K_I for CMP-TEMPO (radical) was calculated as 4.07 mM by the formula $(IC_{50}) * K_M/(K_M + [S])$ [39], and that for CMP-4carboxyTEMPO (radical) was calculated as 0.79 mM. A K_I for CMP-4carboxyTEMPO was also determined from a more extensive investigation of the concentration dependence of activities. The K_I was extracted by using a double-reciprocal Lineweaver-Burk plot and was determined to be 0.75 ± 0.05 mM.

The improvement in affinity of roughly a factor of 5 upon addition of the carboxyl group is consistent with predictions based on expected favorable interactions between the carboxyl group and residues in the active site of ST6Gal I. The affinity for CMP-4carboxyTEMPO is in a range that is expected to be useful in the observation of paramagnetic enhanced relaxation.

Distance-Dependent Line Broadening of ^{15}N HSQC Spectra of ST6Gal I

ST6Gal I can be prepared with ^{15}N enrichment in amide sites of specific amino acids (L.M., J. Glushka, L.H. Stanton, F.T., R.E. Collins, G. Wiley, Z. Gao, J.H.P., and K.W.M., unpublished data). An HSQC spectrum of a 0.3 mM sample prepared with all phenylalanines labeled is presented in Figure 3A. There are 16 phenylalanines in the sequence of the catalytic domain of ST6Gal I, and 16 crosspeaks corresponding to the 16 labeled amide sites are identifiable in Figure 3A. These crosspeaks are not yet assigned to specific sites in the sequence, but strategies are being developed to make these assignments [40]. We can identify crosspeaks belonging to phenylalanines near the CMP-NeuAc-binding site from perturbation of resonances by the bound substrate, bound substrate analogs, or bound product. These were first identified by using the product, CMP. However, it is preferable to use a substrate rather than product for comparison to TEMPO analogs of CMP-NeuAc. The native substrate CMP-NeuAc is unfortunately slowly hydrolyzed during spectral acquisition, so we used a slowly hydrolyzed analog, CMP-3FNeuAc.

A spectrum in the presence of a 10-fold excess of CMP-3FNeuAc is shown in Figure 3B. Unlike many examples of crosspeak perturbation in HSQC spectra by

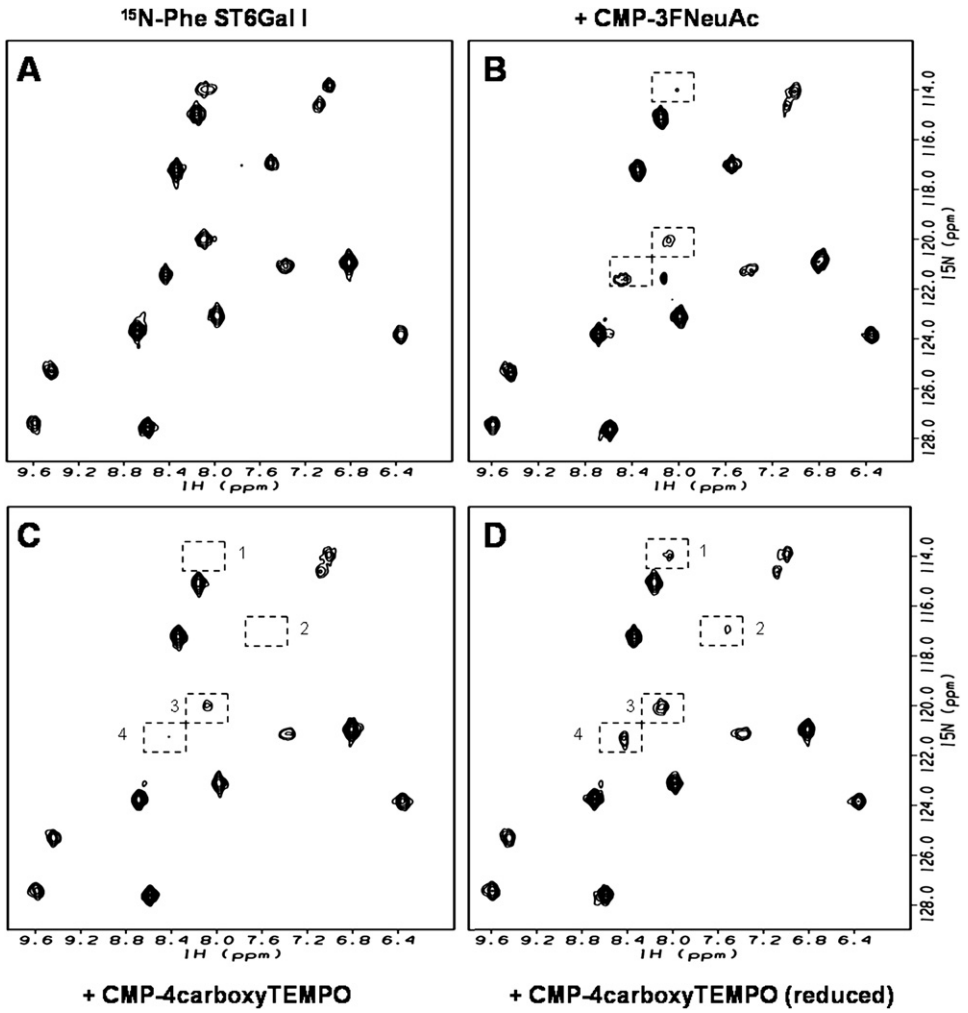

Figure 3. ^{1}H-^{15}N HSQC Spectra of ^{15}N-Phe ST6Gal I in the Presence of CMP-NeuAc Analogs

(A–D) Comparison of ^{1}H-^{15}N HSQC plots of (A) ^{15}N-Phe ST6Gal I, (B) ^{15}N-Phe ST6Gal I with a 10-fold molar excess of CMP-3FNeuAc, and (C and D) ^{15}N-Phe ST6Gal I with a 4-fold excess of CMP-4carboxyTEMPO (C) before and (D) after reduction with a 5-fold excess of ascorbate (relative to the amount of CMP-4carboxyTEMPO). The crosspeaks experiencing changes due to binding dynamics and/or paramagnetic relaxation are boxed.

nonparamagnetic ligands, the dominant effects are broadening or reduction in crosspeak intensity rather than changes in chemical shift. This may be the result of moderately slow exchange, resulting in lifetime broadening of resonances. Substantial induced movement of protein segments upon binding of sugar nucleotides could produce this effect, and this type of motion has been suggested in the studies of several other glycosyltransferases [41].

CMP-TEMPO and CMP-4carboxyTEMPO appear to have qualitatively similar effects as CMP-3FNeuAc on the ^{15}N HSQC of ST6Gal I (Figure 3), which indicates that these analogs very likely bind to the active site with virtually the same protein contacts as the native substrate. Consistent with the difference in binding constants, a 5-fold excess of CMP-TEMPO over CMP-4carboxyTEMPO is required to produce similar levels of perturbation.

In one way, it is unfortunate that crosspeak broadening and an intensity decrease, rather than crosspeak shifts, are seen in the CMP-3FNeuAc spectrum. Multiple contributions to peak broadening can complicate conversion of broadenings to distances between nitroxide- and phenylalanine-labeled sites for the CMP-4carboxyTEMPO spectrum. Fortunately, it is clear that the peaks are more severely perturbed in the presence of CMP-4carboxyTEMPO binding, even with reduced binding to the protein because of its lower binding constant. Also, there is one peak that completely disappears in the presence of CMP-4carboxyTEMPO that was not perturbed by CMP-3FNeuAc. Hence, there is certainly nitroxide-enhanced transverse relaxation present in the presence of CMP-4carboxyTEMPO.

Extraction of nitroxide-dependent paramagnetic effects can be simplified through the use of a better control spectrum. This can be provided based on an ability to remove the effects of paramagnetic perturbation by reduction of the nitroxide to a hydroxylamine. In Figure 3D, one

Table 1. Relative Intensities of the Labeled Crosspeaks in ^{1}H-^{15}N HSQC Regions and Their Corresponding Distance Estimates

Peak Labels	^{15}N-Phe ST6Gal I	With Spin Label	No Spin Label[a]	Distance (Å)
1	1.153 ± 0.046	0.058 ± 0.048	0.374 ± 0.031	10.6–12.9
2	1.239 ± 0.046	0.000 ± 0.048	0.091 ± 0.031	<17.0
3	1.571 ± 0.046	0.562 ± 0.048	0.921 ± 0.031	14.3–15.5
4	1.178 ± 0.046	0.175 ± 0.048	0.440 ± 0.031	12.6–14.4

^{1}H-^{15}N HSQC regions are shown in Figure 3.
[a] Values are taken from the reduced form of CMP-4carboxyTEMPO at a concentration adjusted to compensate for the binding affinity difference between its oxidized form and reduced form.

observes the partial reappearance of the perturbed resonances of the protein when the nitroxide radical is reduced by ascorbate salt. Changes in intensities between reduced and oxidized spectra (Table 1) can then be related to distances between nitroxide- and phenylalanine-labeled positions.

One must also control for the possibility of nonspecific binding to secondary sites. The TEMPO moiety itself is quite hydrophobic and may bind to hydrophobic patches on the protein independently of active site interactions; this can lead to some additional broadening of peaks. To rule this possibility out, a spectrum in the presence of an equivalent amount of 4-carboxy-4-hydroxyTEMPO (**10**) was acquired. No significant crosspeak intensity loss was observed in the spectrum.

Distance Restraints for Molecular Modeling

The difference in intensity of crosspeaks between HSQC spectra of proteins in the presence and absence of a spin-labeled ligand (actually the presence of oxidized and reduced forms) can be used to estimate distances between the position of the nitroxide label in the active site and the protons giving rise to particular crosspeaks. During the transfer and refocusing periods of the experiment, the amide proton magnetization is in the transverse plane and is undergoing intensity loss due to paramagnetic relaxation. A number of authors have employed the following equation to relate the intensity loss to distances between the nitroxide and particular protons [7, 12, 13]:

$$\ln(I_{nsl}/I_{sl}) = f * t * (K/r^6) * (4\tau_c + 3\tau_c * [1 + \omega_H^2\tau_c^2]^{-1}). \quad (1)$$

Here, I_{sl} and I_{nsl} are the peak intensities (measured as peak volumes) of resonances with and without spin label (presence of oxidized and reduced forms), respectively. f is the fraction of protein carrying a ligand, and t (9.52 ms) is the total time during the INEPT (insensitive nuclei enhanced by polarization transfer) and refocusing periods of the HSQC pulse sequence. K is a constant related to spin properties of the system ($K = 1/15*S(S+1)\gamma^2 g^2\beta^2 = 1.23 \times 10^{-32}$ cm^6s^{-2}), r is the distance between the nitroxide and a site giving rise to a crosspeak of interest, τ_c is the effective correlation time for tumbling of the protein, and ω_H (900 MHz* 2π) is the precession frequency for the amide proton. Frequently, a scaling factor that would relate the inverse sixth power of distance to the log of the intensity ratio is calculated empirically by using a known distance in the system. This eliminates the need to independently determine factors appearing in Equation 1. Unfortunately, ST6Gal I does not have a crystal structure, and it is not possible to provide a known distance. We can, however, determine an appropriate scaling factor by using the binding constant determined for the analog (f = 57%), an estimate of the correlation time from spin relaxation data ($\tau_c = 20$ ns), and fundamental nuclear and electron spin constants. The distances resulting from application of Equation 1 are reported in Table 1.

The distances we estimate for the perturbed resonances are all less than 17 Å and well within the bounds of the 25 Å radius expected for a 40 kDa protein. Only an upper limit can be set for peak 2 because of its complete disappearance in the presence of the spin label. Weak intensity in the presence of the reduced spin label also makes the uncertainly in the upper limit to the distance large. Best estimate distances for the other peaks cluster between 10 and 15 Å. The narrow range is the result of the steep $1/r^6$ distance dependence for which a variation in intensity ratios by a factor of two leads to only a 12% variation in distance. We can, in principle, expand the range of sensitivity and improve measurements for peak 2 by collecting data with different concentrations of spin-labeled ligand.

DISCUSSION

The above-described results provide a clear demonstration that nitroxide spin-labeled compounds designed to mimic natural ligands of proteins can be used to obtain structural data on proteins that are difficult to characterize by conventional methods. The data we present require some additional steps before a protein structure can be produced. Crosspeaks must be assigned to specific sites, and this must be done without the aid of experiments that require uniform isotopic labeling. Appropriate methods are being developed [40], but this will take some time. Also, computational methods that use sparse constraints to produce protein structures must be improved [8, 10, 13]. However, the availability of even a few distance

restraints and identification of crosspeaks from residues near the active site are important steps forward.

Prior to completion of a structure for ST6Gal I, we can compare of our distance estimates to distances observed in the crystal structure of related molecules. The bacterial α-2,3-sialyltransferase CstII [19] provides one such comparison. There is very low sequence homology between this protein and ST6Gal I, but programs such as GenTHREADER [42, 43] can predict reasonable sequence alignment. Using this alignment and a model built with MODELER [44], we can predict distances between the nitroxide of bound CMP-4carboxyTEMPO and phenylalanine amide protons. We find the closest four phenylalanine amide protons to be 6.5, 7.8, 11.8, and 16.1 Å from the nitroxide of CMP-4carboxyTEMPO. Considering that one entry is given only as an upper limit, these distances are not far off from those listed in Table 1. In principle, the distances in Table 1 can be used to improve modeling of the ST6Gal 1 structure once sequential assignments of crosspeaks to specific sequential sites in the protein are available.

We can also compare our distances to the rather extensive sequence analysis that has been done for ST6Gal I [45]. Large (L) and small (S) conserved sequence regions have been implicated in binding of the sugar donor. These regions contain three phenylalanines (one in the S motif and two in L motif). This number compares favorably with the number of crosspeaks perturbed in our experiments (four). To our knowledge, our observations thus provide some of the first structural validation of sequences predicted to be involved in sugar nucleotide binding for ST6Gal I.

SIGNIFICANCE

The procedures presented for the synthesis of our spin-labeled CMP-NeuAc analogs produced useful structural probes of ST6Gal I. The analogs are, of course, applicable to other sialyltransferases. There are some 411 sialyltransferases identified in the CAZY database, and all are believed to use the same CMP-NeuAc sugar donor. The synthetic approach is also potentially applicable to the preparation of probes for other glycosyltransferases. Here, there are thousands of entries distributed among 87 families, but there are only a few commonly used sugar donors. This makes a limited set of spin-labeled compounds broadly applicable to a large class of structural problems.

Structure determination of uncharacterized proteins from sparse label constraints is, as yet, not widely practiced. However, the potential importance in difficult structural problems, such as those involving membrane proteins [46] and multiprotein complexes, is clearly recognized [47, 48]. New methods for predicting structures from sparse constraints have also begun to appear. These have used sparse distance constraints from a variety of other sources, including chemical crosslinking, backbone to backbone NOEs, and paramagnetic metal ion perturbations [49–52], but distance constraints coming from nitroxide spin-labeled perturbations can be used in a very similar way. Glycosylated proteins represent a new structural challenge in which information from sparse labels may be the only type of information accessible. Hence, the methods derived for structural analysis of ST6Gal I, itself a glycosylated protein, should find numerous applications to other proteins in the future.

EXPERIMENTAL PROCEDURES

Synthesis of CMP-TEMPO, 1, and CMP-4CarboxyTEMPO, 2

General Procedures

Chemicals and dry solvents were purchased from Aldrich (USA). The commercial 4-oxo-TEMPO was purified by chromatography (silica gel, 82:18 hexanes:EtOAc). All moisture-sensitive reactions were performed under an atmosphere of dry argon. Reactions were monitored by TLC on silica gel Kieselgel 60 F_{254} (Merck) and were visualized under UV light and by charring with a ceric ammonium molybdate reagent. All evaporations were performed under appropriate reduced pressure at a bath temperature < 30°C. Chromatography was performed on silica gel Merck 70-230 mesh or, as indicated, on Iatrobeads 6RS-8060 (60 μm, Bioscan), or, for reverse phase, on a Waters preparative C18 WAT020594 column (125 Å, 55–105 μm). All NMR spectra of the TEMPO derivatives were acquired on Varian 300, 500, or 600 MHz NMR spectrometers, in the indicated solvents, after addition of phenyl hydrazine as a reducing agent to the nitroxide sample [53]. Mass spectra were obtained on an Applied Biosystems Voyager-DE MALDI-TOF mass spectrometer by using DHB (2,5-dihydroxybenzoic acid) as a matrix.

2-Cyanoethyl 1-Oxyl-2,2,6,6-Tetramethylpiperidin-4-yl N,N-Diisopropyl Phosphoramidite, 4

For more information, see [33]. Diisopropylethylammine (297 mg, 2.30 mmol) was added to a solution of 4-hydroxy-TEMPO, **3** (198 mg, 1.15 mmol), and 2-cyanoethyl N,N-diisopropylchlorophosphoramidate (407 mg, 1.72 mmol) in dry CH_2Cl_2 (5 ml) cooled at 0°C under an argon atmosphere. The mixture was then stirred for 1 hr at room temperature until TLC (3:1 hexanes:EtOAc) indicated the completion of the reaction. The solvent was coevaporated with toluene, and the residue was purified by flash chromatography (8 g Iatrobeads, 4:1:0.2% hexanes:EtOAc:NEt_3) to afford **4** (164 mg, 38%) as an orange syrup (R_f 0.7, 3:1 hexanes:EtOAc). No NMR data are available for **4** due to the rapid decomposition observed in the NMR tube after addition of phenyl hydrazine. MS data are not available for **4** due to its instability in the matrix.

2-Cyanoethyl (2′,3′-O,N^4-Triacetylcytidin-5′-yl) 1-Oxyl-2,2,6,6-Tetramethylpiperidinyl-4-yl Phosphate, 6

For more information, see [32]. Compounds **4** and **5** [31] were separately dried by coevaporating three times with dry toluene. Tetrazole (1 ml of a 3% solution in MeCN) was slowly syringed into a mixture of phosphoramidite, **4** (160 mg, 0.43 mmol), and the cytidine **5** (125 mg, 0.38 mmol) in MeCN (2 ml) at 0°C. The reaction was followed by TLC (95:5 $CHCl_3$:MeOH) and seemed complete after stirring for about 1 hr at room temperature. After the addition of three drops of triethylamine, the solvents were coevaporated with toluene, providing an orange material (0.30 g) that was used in the next step without purification. A 5.5 M solution of tBuOOH in decane (0.47 ml) was slowly added to the crude material (0.27 g) dissolved in MeCN (4 ml) while stirring in ice. The reaction was followed by TLC (95:5 $CHCl_3$:MeOH). After 1 hr, the mixture was diluted with EtOAc and was washed with a saturated $NaHCO_3$ solution followed by brine. After drying over $MgSO_4$, the solvent was evaporated, and the residue was purified by chromatography (5 g Iatrobeads, 97:3 $CHCl_3$:MeOH) to afford the orange product, **6** (160 mg, 64%), as a 1:1 diastereoisomeric mixture (R_f 0.4, 95:5

$CHCl_3$:MeOH). ^1H NMR (500 MHz, CD_3OD) for the reduced form: δ 8.13 (d, J = 7.0 Hz, 1H, H-6), 8.11 (d, J = 7.5 Hz, 1H, H-6), 7.48–7.40 (m, 2H, 2 × H-5), 6.03–6.02 (m, 2H, 2 × H-1′), 5.52–5.44 (m, 4H, 2 × 2H of H-2′ and H-3′), 4.74–4.68 (m, 2H, 2 × H-1″), 4.48–4.41 (m, 4H, 2 × 2H of H-4′ and H-5′), 4.40–4.33 (m, 2H, H-5′), 4.30 (p, J = 6.5 Hz, 4H, 2 × CH_2CN), 2.95–2.86 (m, 4H, 2 × $OC\underline{H}_2CH_2CN$), 2.18 (s, 6H, 2 × CH_3CO), 2.10 (d, J = 2 Hz, 12H, 4 × CH_3CO), 2.10–2.01 (m, 4H, 2 × 2H of H-3″ and H-5″), 1.70–1.61 (m, 4H, 2 × 2H of H-3″ and H-5″), 1.22–1.10 (m, 24H, 8 × CH_3); MALDI-TOF/MS: (M + Na^+) m/z 679.4, calcd for $C_{27}H_{39}N_5O_{12}PNa$ 679.2225.

CMP-TEMPO, 1

For more information, see [32]. 1,8-Diazabicyclo[5,4,0]-7-undecene (DBU) (2.7 mg, 0.018 mmol) was added to a solution of the above-described material, **6** (10 mg, 0.015 mmol), in THF (0.8 ml), and the mixture was stirred at room temperature for 45 min until TLC (95:5 $CHCl_3$:MeOH) indicated the completion of the reaction. A 5.4 M solution of NaOMe in MeOH (0.028 ml, 0.15 mmol) and then a mixture of 1:2 MeOH:H_2O (1.5 ml) were added to this mixture. After stirring for 12 hr at room temperature, the mixture was lyophilized, providing a residue that was then loaded onto a small column of reverse-phase C18 eluted with water to remove NaOH and NaOAc, and then run through a small column of Bio-Rad AG 50W-X8 Na^+ eluted with water to remove the DBU byproduct. After freeze drying, the recovered material was purified by size-exclusion chromatography on Bio-Gel P2 (extra fine, 1.5 cm × 45 cm, water, 4°C) and lyophilization to provide CMP-TEMPO, **1** (5.5 mg, 73%), as a yellow powder (5:2 iPrOH:0.5 M AcOH•NEt_3, R_f 0.7; HPTLC RP-18 WF_{254S}, R_f 0.2, water). ^1H NMR (500 MHz, CD_3OD) for the reduced form: δ 8.11 (d, J = 7.5 Hz, 1H, H-6), 5.99–5.96 (m, 2H, H-5 and H-1′), 4.49–4.38 (m, 1H, H-1″), 4.28–4.00 (m, 5H, H-3′, H-5′, H-2′, H-4′, and H-5′), 1.80–1.71 (m, 2H, H-3″ and H-5″), 1.56 (td, J = 3.5, 12.0 Hz, 2H, H-3″ and H-5″), 1.15 (s, 3H, CH_3), 1.13 (s, 6H, 2 × CH_3), 1.09 (s, 3H, CH_3); ^{31}P NMR (500 MHz, CD_3OD, external standard H_3PO_4 = 0.00) δ 0.72; ^{13}C NMR (500 MHz, CD_3OD) for the reduced form: δ 167.1 (C-2), 158.1 (C-NH_2), 142.5 (C-6), 96.0 (C-5), 90.7 (C-1′), 83.9 (d, J = 8.8, C-4′), 75.9 (C-2′), 70.2 (C-3′), 68.8 (d, J = 6.0, C-4″), 64.5 (d, J = 5.5, C-5′), 59.6 (C-2″ and C-6″), 46.9 (d, J = 4.0, C-3″/C-5″), 46.8 (d, J = 4.0, C-3″/C-5″), 32.2 (CH_3), 20.4 (CH_3); MALDI-TOF/MS for the reduced form: (M + Na^+) m/z 501.3, calcd for $C_{18}H_{31}N_4O_9PNa$ 501.1721.

1,4-Dihydroxy 2,2,6,6-Tetramethyl-4-Piperidinecarboxylic Acid, 9

For more information, see [36]. A solution of the cyanide **8** [35] (1.07 g, 5.35 mM) in 27% HCl (4.8 ml) was stirred for 2 hr at 80°C. Coevaporation with 80 ml water under reduced pressure (bath temperature < 30°C) left an acidic, yellowish, oily solid that was left at −20°C overnight. The acidic supernatant was pipetted off, and the residual solid was washed three times with ether and further dried in vacuo to yield the crude N-hydroxyde **9** (750 mg). ^1H NMR (300 MHz, D_2O): δ 2.38 (d, J = 14.9 Hz, 2H, H-3, and H-5), 2.20 (d, J = 14.9 Hz, 2H, H-3, and H-5), 1.635 (s, 6H, 2 × CH_3), 1.428 (s, 6H, 2 × CH_3). MALDI-TOF/MS: (M + Na^+) m/z 240.1, calcd for $C_{10}H_{19}NO_4Na$ 240.1206. The material, **9**, was taken to the next step without further purification.

4-Hydroxy-4-Methoxycarbonyl-1-Oxyl-2,2,6,6-Tetramethylpiperidine, 10

A solution of diazomethane in ether was added to a solution of crude **9** (750 mg) in MeOH (10 ml) at 0°C until the solution became deep yellow. The mixture was then stirred in an open flask for 2 days [37, 38]. Formation of the nitroxide (upper spot) was followed by TLC (95:5 $CHCl_3$:MeOH), and a small amount of N-hydroxyl starting material remained untransformed. Purification by chromatography (20 g Iatrobeads, 99:1 $CHCl_3$:MeOH) gave **10**, which was further purified by crystallization from a mixture of ether and hexanes at −20°C, providing **10** (684 mg, 55%) as orange crystals (R_f 0.4, 3:1 hexanes:EtOAc). ^1H NMR (300 MHz, CD_3OD) for the reduced form: δ 3.71 (s, 3H, CH_3OCO), 2.04 (d, J = 13.6 Hz, 2H, H-3, and H-5), 1.80 (d, J = 13.6 Hz, 2H, H-3, and H-5), 1.35 (s, 6H, 2 × CH_3), 1.16 (s, 6H, 2 × CH_3); MALDI-TOF/MS for the reduced form: (M + Na^+) m/z 254.1, calcd for $C_{11}H_{21}NO_4Na$ 254.1363.

2-Cyanoethyl 4-Methoxycarbonyl-1-Oxyl-2,2,6,6-Tetramethylpiperidin-4-yl) N,N-Diisopropylphosphoramidite, 11

For more information, see [33]. Diisopropylethylammine (168 mg, 1.30 mmol) was added to a solution of the above-described TEMPO derivative, **10** (150 mg, 0.65 mmol), and 2-cyanoethyl N,N-diisopropyl-chlorophosphoramidate (231 mg, 0.98 mmol) in dry CH_2Cl_2 (2 ml) cooled at 0°C under an argon atmosphere. The mixture was then stirred for 24 hr at room temperature until TLC (3:1 hexanes:EtOAc) indicated the completion of the reaction. The solvent was coevaporated with toluene, and the residue was purified by flash chromatography (5 g Iatrobeads, 4:1:0.2% hexanes:EtOAc:NEt_3) to afford **11** (240 mg, 86%) as a brown syrup (R_f 0.5, 3:1 hexanes:EtOAc). ^1H NMR (300 MHz, CD_3OD) for the reduced form: δ 3.77–3.66 (m, 4H, $OC\underline{H}_2CH_2CN$ and 2 × $C\underline{H}$ $(CH_3)_2$), 3.71 (s, 3H, CH_3OCO), 2.67 (t, J = 5.9 Hz, 2H, CH_2CN), 2.25–1.87 (m, 4H, H-3, and H-5), 1.33–1.12 (m, 24H, 8 × CH_3). No MS data are available for **11** due to its rapid decomposition in the matrix.

2-Cyanoethyl 2′,3′-O,N^4-Triacetylcytidin-5′-yl 4-Carboxy-1-Oxyl-2,2,6,6-Tetramethylpiperidin-4-yl Phosphate, 12

For more information, see [32]. Compounds **5** [31] and **11** were dried by coevaporating two times with dry toluene. Tetrazole (0.7 ml, 0.45 M solution in MeCN) was then syringed into a mixture of phosphoramidite, **11** (80 mg, 0.186 mmol), and the cytidine **5** (75 mg, 0.203 mmol) in MeCN (2.5 ml) cooled at −40°C. After 5 min, the reaction mixture was brought to room temperature and was stirred with one weight equivalent of activated, crushed 3 Å molecular sieves for 2 hr. The reaction was followed by TLC (9:1 EtOAc:MeOH). A 5.5 M solution of tBuOOH in decane (0.8 ml) was then added directly to the crude mixture at 0°C. The reaction was monitored by TLC (9:1 EtOAc:MeOH). After 1 hr, the mixture was diluted with EtOAc and washed with a saturated $NaHCO_3$ solution and brine. After drying over $MgSO_4$, the solvent was evaporated and the residue was purified by size-exclusion chromatography on Sephadex LH-20 (2.5 × 45 cm) by using MeOH as eluent to give the phosphate **12** (53 mg, 40%) as a 1:1 diastereomeric mixture (R_f 0.3, 9:1 EtOAc:MeOH). ^1H NMR (300 MHz, CD_3OD) for the reduced form: δ 8.17 (d, J = 7.6 Hz, 1H, H-6), 8.16 (d, J = 7.6 Hz, 1H, H-6), 7.49 (d, J = 7.5 Hz, 1H, H-5), 7.48 (d, J = 7.5 Hz, 1H, H-5), 6.06 (d, J = 6.3 Hz, 1H, H-1′), 6.04 (d, J = 6.3 Hz, 1H, H-1′), 5.51–5.48 (m, 4H, 2 × 2H of H-2′ and H-3′), 4.60–4.40 (m, 6H, 2 × 3H of H-4′ and H-5′), 4.34 (q, J = 6.13 Hz, 4H, 2 × CH_2CN), 3.79 (s, 6H, 2 × CH_3OCO), 2.89–2.86 (m, 4H, 2 × $OC\underline{H}_2CH_2CN$), 2.22–2.06 (m, 8H, 2 × 4H of H-3″ and H-5″), 2.17 (s, 6H, 2 × CH_3CO), 2.10 (d, J = 1.9 Hz, 12H, 4 × CH_3CO), 1.33–1.29 (m, 12H, 4 × CH_3), 1.17 (s, 12H, 4 × CH_3); MALDI-TOF/MS for the reduced form: (M + Na^+) m/z 738.1, calcd for $C_{29}H_{42}N_5O_{14}PNa$ 738.2358.

CMP-4CarboxyTEMPO, 2

For more information, see [32]. 1,8-Diazabicyclo[5,4,0]-7-undecene (14.7 mg, 0.096 mmol) was added to a solution of the above-described material, **12** (53 mg, 0.074 mmol), in THF (0.8 ml), and the mixture was stirred at room temperature for 1 hr until TLC (9:1 EtOAc:MeOH) indicated the completion of the reaction. A 5.4 M solution of NaOMe in MeOH (0.083 ml, 0.45 mmol) and then a mixture of 1:2 MeOH:H_2O (1.5 ml) were added to this mixture. After stirring for 9 hr at room temperature, the mixture was lyophilized. The residue was loaded onto a small column of reverse-phase C18, eluted with water to remove NaOH and NaOAc, and then run through a small column of Bio-Rad AG 50W-X8 Na^+ eluted with water to remove the DBU byproduct. After freeze drying, the recovered material was purified by size-exclusion chromatography on Bio-Gel P2 (extra fine, 1.5 cm × 45 cm, water, at 4°C) and lyophilization to provide CMP-4carboxyTEMPO, **2** (31 mg, 74%), as a yellow powder (5:2 iPrOH:0.5 M AcOH•NEt_3, R_f 0.5; HPTLC RP-18 WF_{254S}, R_f 0.4, water). ^1H NMR (600 MHz, CD_3OD) for the reduced form: δ 8.22 (d, J = 7.8 Hz, 1H, H-6), 6.12 (d, J = 7.8 Hz, 1H, H-5), 5.97 (d, J = 3.0 Hz, 1H, H-1′), 4.39 (t, J = 5.5 Hz, 1H, H-3′), 4.32–4.24 (m, 1H, H-5′), 4.24–4.18 (m, 1H, H-5′), 4.17–4.10 (m, 2H, H-2′, and H-4′), 2.51 (d, J = 14.6 Hz, 1H, H-3″, or H-5″), 2.40 (d, J = 14.6 Hz, 1H, H-3″, or H-5″), 2.21 (t, J = 14.8 Hz, 2H, H-3″, and H-5″), 1.44 (d, J = 13.8 Hz, 6H, 2 × CH_3), 1.23 (s, 6H,

2 × CH_3); ^{13}C NMR (500 MHz, CD_3OD) for the reduced form: δ 181.6 (COOH), 167.2 (C-2), 158.1 (C-NH_2), 142.8 (C-6), 96.1 (C-5), 90.9 (C-1′), 84.0 (C-4′), 76.0 (C-2′), 69.6(C-3′), 64.2 (C-5′), 59.3 (C-2″ and C-6″), 45.8 (C-3″ and C-5″), 31.6 (CH_3), 22.8 (CH_3); ^{31}P NMR (500 MHz, CD_3OD, H_3PO_4 external standard = 0.00) δ 0.13; MALDI-TOF/MS for the reduced form: (M + Na^+) m/z 545.6, calcd for $C_{19}H_{31}N_4O_{11}PNa$ 545.1619.

Production of ^{15}N-Phe ST6Gal I

An NH_2-terminal His-tagged form of the rat ST6Gal I catalytic domain (residues 97–403 from GenBank P13721) [21] was expressed in mammalian HEK293 cells in the pEAK expression vector (Edge Biosystems, Gaithersburg, MD). Transfected cells were grown at 37°C in DMEM medium supplemented with 10% FBS and 1 μg/ml puromycin for antibiotic selection. When the cells had grown to 70% confluency, they were subcultured at a 1:5 ratio and grown to confluency in DMEM media depleted of Phe and supplemented with 2-fold excess (132 mg/L) ^{15}N-Phe, 10% dialyzed FBS, and 1 μg/ml puromycin. After growth to confluency, the culture media was harvested, and ST6Gal I was purified sequentially over Phenyl Sepharose, Ni-NTA, and Superdex-75 columns. The purified protein was stored in 20 mM Bis-Tris (pH 6.5), 200 mM NaCl buffer. A detailed description of the recombinant ST6Gal I expression in HEK293 cells, ^{15}N-Phe labeling, and purification will be published separately (L.M., J. Glushka, L.H. Stanton, F.T., R.E. Collins, G. Wiley, Z. Gao, J.H.P., and K.W.M., unpublished data).

Activity and Inhibition Assays

The activity of ST6Gal I was determined by a radioactive assay based on the transfer of [^{14}C] sialic acid from a CMP-[^{14}C] sialic acid donor to an N-acetyllactosamine acceptor [54]. The buffer used in the assay was sodium cacodylate (50 mM, pH 6.5) containing 0.1% (v/v) Triton X-100 and 0.2 mg/ml BSA, and assays were performed at 37°C for 15 min. The sialylated product was isolated by ion-exchange chromatography on Dowex 1-X 8 (0.8 × 3 cm) columns and was counted with a scintillation counter (BECKMAN LS 5000TD).

For IC_{50} measurements, reaction mixtures consisted of 2.1 mM CMP-NeuAc, 9.2 nM CMP-[^{14}C] NeuAc as tracer, 4.4 mM LacNAc (N-acetyllactosamine), 11.1 nmol ST6Gal I, and inhibitor CMP-TEMPO (0–17 mM) or CMP-4carboxyTEMPO (0–6 mM). For Ki measurement on CMP-4carboxyTEMPO, another series of reaction mixtures was prepared with 9.2 nM CMP-[^{14}C] NeuAc, 4.4 mM LacNAc, 11.1 nmol ST6Gal I, CMP-NeuAc (9–171 μM), and inhibitor (0, 0.8, 1.6, 2.4, and 3.2 mM) in a total volume of 60 μl. A K_i was extracted by using a double-reciprocal Lineweaver-Burk plot.

Collection of NMR Spectra

NMR samples were prepared in 10% D_2O/90% Bis-Tris buffer (20 mM) at pH 6.5 with the protein concentration at 0.3 mM. The protein itself is soluble to a higher level, but it appears to form dimers or higher oligomers above this concentration, resulting in severe loss of signal. Spectra were acquired on a Varian INOVA spectrometer operating at 900 MHz for protons. The spectrometer was equipped with a triple-resonance cryogenic probe with z-pulsed gradient coils. Spectra were run with the fast HSQC sequence supplied as part of the Varian BioPak. Data were typically acquired with 11990 Hz as SW, 1800 Hz as SW1, 48 indirect t1 complex points and 514 direct t2 complex points, and a recycling rate of 1.5 s. Each spectrum represents a total acquisition time of about 3 hr for 64 scans.

ACKNOWLEDGMENTS

This work was supported by a grant from the National Center for Research Resources of the National Institutes of Health (NIH) (RR05351) in support of the Research Resource for Integrated Glycotechnology, by a research grant from the National Institute of General Medical Sciences (GM033225), and a grant from the National Institute of General Medicine of the NIH (GM066340) in support of the Southeast Collaboratory for High Field NMR. We thank Laura Morris for her help in ST6Gal I modeling.

Received: November 1, 2006
Revised: February 14, 2007
Accepted: February 27, 2007
Published: April 27, 2007

REFERENCES

1. Moseley, H.N.B., Monleon, D., and Montelione, G.T. (2001). Automatic determination of protein backbone resonance assignments from triple resonance nuclear magnetic resonance data. Methods Enzymol. *339*, 91–108.
2. Wider, G. (2005). NMR techniques used with very large biological macromolecules in solution. Methods Enzymol. *394*, 382–398.
3. Lustbader, J.W., Birken, S., Pollak, S., Pound, A., Chait, B.T., Mirza, U.A., Ramnarain, S., Canfield, R.E., and Brown, J.M. (1996). Expression of human chorionic gonadotropin uniformly labeled with NMR isotopes in Chinese hamster ovary cells: an advance toward rapid determination of glycoprotein structures. J. Biomol. NMR *7*, 295–304.
4. Mao, H.Y., Gunasekera, A.H., and Fesik, S.W. (2000). Expression, refolding, and isotopic labeling of human serum albumin domains for NMR spectroscopy. Protein Expr. Purif. *20*, 492–499.
5. Varki, A. (1993). Biological roles of oligosaccharides: all of the theories are correct. Glycobiology *3*, 97–130.
6. Bruggert, M., Rehm, T., Shanker, S., Georgescu, J., and Holak, T.A. (2003). A novel medium for expression of proteins selectively labeled with N-15-amino acids in *Spodoptera frugiperda* (Sf9) insect cells. J. Biomol. NMR *25*, 335–348.
7. Battiste, J.L., and Wagner, G. (2000). Utilization of site-directed spin labeling and high-resolution heteronuclear nuclear magnetic resonance for global fold determination of large proteins with limited nuclear Overhauser effect data. Biochemistry (Mosc.) *39*, 5355–5365.
8. Gaponenko, V., Howarth, J.W., Columbus, L., Gasmi-Seabrook, G., Yuan, J., Hubbell, W.L., and Rosevear, P.R. (2000). Protein global fold determination using site-directed spin and isotope labeling. Protein Sci. *9*, 302–309.
9. Gillespie, J.R., and Shortle, D. (1997). Characterization of long-range structure in the denatured state of staphylococcal nuclease. 1. Paramagnetic relaxation enhancement by nitroxide spin labels. J. Mol. Biol. *268*, 158–169.
10. Gillespie, J.R., and Shortle, D. (1997). Characterization of long-range structure in the denatured state of staphylococcal nuclease. 2. Distance restraints from paramagnetic relaxation and calculation of an ensemble of structures. J. Mol. Biol. *268*, 170–184.
11. Jahnke, W. (2002). Spin labels as a tool to identify and characterize protein-ligand interactions by NMR spectroscopy. ChemBioChem *3*, 167–173.
12. Jain, N.U., Venot, A., Umemoto, K., Leffler, H., and Prestegard, J.H. (2001). Distance mapping of protein-binding sites using spin-labeled oligosaccharide ligands. Protein Sci. *10*, 2393–2400.
13. Johnson, P.E., Brun, E., MacKenzie, L.F., Withers, S.G., and McIntosh, L.P. (1999). The cellulose-binding domains from *Cellulomonas fimi* β-1,4-glucanase CenC bind nitroxide spin-labeled cellooligosaccharides in multiple orientations. J. Mol. Biol. *287*, 609–625.
14. Kuliopulos, A., Westbrook, E.M., Talalay, P., and Mildvan, A.S. (1987). Positioning of a spin-labeled substrate-analog into the structure of delta-5-3-ketosteroid isomerase by combined kinetic, magnetic-resonance, and X-ray-diffraction methods. Biochemistry (Mosc.) *26*, 3927–3937.

15. Schmidt, P.G., and Kuntz, I.D. (1984). Distance measurements in spin-labeled lysozyme. Biochemistry (Mosc.) *23*, 4261–4266.
16. Jamieson, J.C. (1988). Studies on the effect of 1-deoxynojirimycin on the release of albumin, sialyltransferase and α-1 acid glycoprotein from liver slices from normal and inflamed rats. Life Sci. *43*, 691–697.
17. Dall'Olio, F., and Chiricolo, M. (2001). Sialyltransferases in cancer. Glycoconj. J. *18*, 841–850.
18. Hennet, T., Chui, D., Paulson, J.C., and Marth, J.D. (1998). Immune regulation by the ST6Gal sialyltransferase. Proc. Natl. Acad. Sci. USA *95*, 4504–4509.
19. Chiu, C.P.C., Watts, A.G., Lairson, L.L., Gilbert, M., Lim, D., Wakarchuk, W.W., Withers, S.G., and Strynadka, N.C.J. (2004). Structural analysis of the sialyltransferase CstII from *Campylobacter jejuni* in complex with a substrate analog. Nat. Struct. Mol. Biol. *11*, 163–170.
20. Ni, L.S., Sung, M.C., Yu, H., Chokhawala, H., Chen, X., and Fisher, A.J. (2006). Cytidine 5′-monophosphate (CMP)-induced structural changes in a multifunctional sialyltransferase from *Pasteurella multocida*. Biochemistry (Mosc.) *45*, 2139–2148.
21. Weinstein, J., Lee, E.U., Mcentee, K., Lai, P.H., and Paulson, J.C. (1987). Primary structure of β-Galactoside α-2,6-sialyltransferase. Conversion of membrane-bound enzyme to soluble forms by cleavage of the Nh2-terminal signal anchor. J. Biol. Chem. *262*, 17735–17743.
22. Hamamoto, T., Kurosawa, N., Nakaoka, T., Lee, Y.C., Kawasaki, M., and Tsuji, S. (1993). Expression of mouse β-Galactoside α-2,6-sialyltransferase in an insoluble form in *Escherichia coli* and partial renaturation. Glycoconj. J. *10*, 236–237.
23. Wang, X.F., Zhang, L.H., and Ye, X.S. (2003). Recent development in the design of sialyltransferase inhibitors. Med. Res. Rev. *23*, 32–47.
24. Dufner, G., Schworer, R., Muller, B., and Schmidt, R.R. (2000). Base- and sugar-modified cytidine monophosphate N-acetylneuraminic acid (CMP-Neu5Ac) analogues - Synthesis and studies with α(2-6)-sialyltransferase from rat liver. Eur. J. Org. Chem. *8*, 1467–1482.
25. Watts, A.G., and Withers, S.G. (2004). The synthesis of some mechanistic probes for sialic acid processing enzymes and the labeling of a sialidase from *Trypanosoma rangeli*. Can. J. Chem. *82*, 1581–1588.
26. Sosnovsky, G., and Konieczny, M. (1976). Phosphorylative spin-labeling of amino-acids and steroids. Synthesis *8*, 537–539.
27. Sosnovsky, G., and Konieczny, M. (1977). Novel transfer-reactions of a nitroxyl-labeled phosphoryl moiety. Synthesis *9*, 618–619.
28. Cocco, L., and Blakley, R.L. (1979). Synthesis of a spin-labeled analog of nicotinamide adenine-dinucleotide phosphate and its interaction with dihydrofolate-reductase. Biochemistry (Mosc.) *18*, 2414–2419.
29. Weiner, H. (1969). Interaction of a spin-labeled analog of nicotinamide-adenine dinucleotide with alcohol dehydrogenase. I. Synthesis kinetics and electron paramagnetic resonance studies. Biochemistry (Mosc.) *8*, 526–533.
30. Claesen, C.A.A., Daemen, C.J.M., and Tesser, G.I. (1986). Synthesis of spin-labeled Di-2-deoxyadenylates and Tri-2-deoxyadenylates. Recueil Des Travaux Chimiques Des Pays-Bas *105*, 116–123.
31. Chappell, M.D., and Halcomb, R.L. (1997). Synthesis of CMP-sialic acid conjugates: substrates for the enzymatic synthesis of natural and designed sialyl oligosaccharides. Tetrahedron *53*, 11109–11120.
32. Kajihara, Y., Ebata, T., Koseki, K., Kodama, H., Matsushita, H., and Hashimoto, H. (1995). Efficient chemical synthesis of Cmp-Neu5ac and Cmp-(Neu5ac-α-2-]-8neu5ac). J. Org. Chem. *60*, 5732–5735.
33. Kondo, H., Ichikawa, Y., and Wong, C.H. (1992). β-Sialyl phosphite and phosphoramidite: synthesis and application to the chemoenzymatic synthesis of Cmp-sialic acid and sialyl oligosaccharides. J. Am. Chem. Soc. *114*, 8748–8750.
34. Schaub, C., Muller, B., and Schmidt, R.R. (2000). Sialyltransferase inhibitors based on CMP-quinic acid. Eur. J. Org. Chem. *2000*, 1745–1758.
35. Wong, L.T.L., Schwenk, R., and Hsia, J.C. (1974). New synthesis of nitroxyl radicals of piperidine and tetrahydropyridine series. Can. J. Chem. *52*, 3381–3383.
36. Avi, M., Fechter, M.H., Gruber, K., Bela, F., Pochlauer, P., and Griengl, H. (2004). Hydroxynitrile lyase catalysed synthesis of heterocyclic (R)- and (S)-cyanohydrins. Tetrahedron *60*, 10411–10418.
37. Dulog, L., and Wang, W. (1992). A bisnitroxyl dipeptide. Liebigs Ann. Chem. *4*, 301–303.
38. Galera, E., Szykula, J., and Zabza, A. (1987). Insect growth-regulators. 19. Synthesis of farnesyl-type juvenoids with a tetramethylpiperidinoxyl marker. Liebigs Ann. Chem. *9*, 777–780.
39. Voet, D., and Voet, J.G. (2004). Biochemistry, Third Edition (Hoboken, NJ: John Wiley & Sons, Inc.).
40. Feng, L.M., Orlando, R., and Prestegard, J.H. (2006). Amide proton back-exchange in deuterated peptides: applications to MS and NMR analyses. Anal. Chem. *78*, 6885–6892.
41. Gordon, R.D., Sivarajah, P., Satkunarajah, M., Ma, D., Tarling, C.A., Vizitiu, D., Withers, S.G., and Rini, J.M. (2006). X-ray crystal structures of rabbit N-acetylglucosaminyltransferase I (GnT I) in complex with donor substrate analogues. J. Mol. Biol. *360*, 67–79.
42. Jones, D.T. (1999). GenTHREADER: an efficient and reliable protein fold recognition method for genomic sequences. J. Mol. Biol. *287*, 797–815.
43. McGuffin, L.J., and Jones, D.T. (2003). Improvement of the GenTHREADER method for genomic fold recognition. Bioinformatics *19*, 874–881.
44. Marti-Renom, M.A., Stuart, A.C., Fiser, A., Sanchez, R., Melo, F., and Sali, A. (2000). Comparative protein structure modeling of genes and genomes. Annu. Rev. Biophys. Biomol. Struct. *29*, 291–325.
45. Jeanneau, C., Chazalet, V., Auge, C., Soumpasis, D.M., Harduin-Lepers, A., Delannoy, P., Imberty, A., and Breton, C. (2004). Structure-function analysis of the human sialyltransferase ST3Gal I: role of N-glycosylation and a novel conserved sialylmotif. J. Biol. Chem. *279*, 13461–13468.
46. Brown, W.M., Faulon, J.L., and Sale, K. (2005). A deterministic algorithm for constrained enumeration of transmembrane protein folds. Comput. Biol. Chem. *29*, 143–150.
47. Tang, C., and Clore, G.M. (2006). A simple and reliable approach to docking protein-protein complexes from very sparse NOE-derived intermolecular distance restraints. J. Biomol. NMR *36*, 37–44.
48. Ye, X.D., O'Neil, P.K., Foster, A.N., Gajda, M.J., Kosinski, J., Kurowski, M.A., Bujnicki, J.M., Friedman, A.M., and Bailey-Kellogg, C. (2004). Probabilistic cross-link analysis and experiment planning for high-throughput elucidation of protein structure. Protein Sci. *13*, 3298–3313.
49. Barbieri, R., Luchinat, C., and Parigi, G. (2004). Backbone-only protein solution structures with a combination of classical and paramagnetism-based constraints: a method that can be scaled to large molecules. ChemPhysChem *5*, 797–806.
50. Kim, D.E., Chivian, D., and Baker, D. (2004). Protein structure prediction and analysis using the Robetta server. Nucleic Acids Res. *32*, W526–W531.
51. Li, W., Zhang, Y., and Skolnick, J. (2004). Application of sparse NMR restraints to large-scale protein structure prediction. Biophys. J. *87*, 1241–1248.

52. Qu, Y.X., Guo, J.T., Olman, V., and Xu, Y. (2004). Protein structure prediction using sparse dipolar coupling data. Nucleic Acids Res. *32*, 551–561.

53. Lee, T.D., and Keana, F.W. (1975). Insitu reduction of nitroxide spin labels with phenylhydrazine in deuteriochloroform solution: convenient method for obtaining structural information on nitroxides using nuclear magnetic-resonance spectroscopy. J. Org. Chem. *40*, 3145–3147.

54. Sadler, J.E., Beyer, T.A., Oppenheimer, C.L., Paulson, J.C., Prieels, J.P., Rearick, J.I., and Hill, R.L. (1982). Purification of mammalian glycosyltransferases. Methods Enzymol. *83*, 495–496.

